http://www.jstage.jst.go.jp/browse/biophysics

BIOPHYSICS

Vol. 10, pp. 77–88 (2014)
doi: 10.2142/biophysics.10.77

Morphological and physiological characteristics of dermal photoreceptors in *Lymnaea stagnalis*

Satoshi Takigami[1,2], Hiroshi Sunada[3], Tetsuro Horikoshi[1,2,4], Manabu Sakakibara[1,2,5]

[1]*Graduate School of High-Technology for Human Welfare, Tokai University, Numazu, Shizuoka 410-0321, Japan*
[2]*Graduate School of Bioscience, Tokai University, Numazu, Shizuoka 410-0321, Japan*
[3]*Hotchkiss Brain Institute, Faculty of Medicine, University of Calgary, Calgary, AB T2N 4N1, Canada*
[4]*School of Engineering, Department of Biomedical Engineering, Tokai University, Hiratsuka, Kanagawa 259-1292, Japan*
[5]*School of High-Technology for Human Welfare, Tokai University, Numazu, Shizuoka 410-0321, Japan*

Received September 5, 2014; accepted October 14, 2014

Dermal photoreceptors located in the mantle of *Lymnaea stagnalis* were histologically and physiologically characterized. Our previous study demonstrated that the shadow response from dermal photoreceptors induces the whole-body withdrawal response. Through the interneuron, RPeD11, we detected that the light-off response indirectly originated from a dermal photoreceptor. Previous observations, based on behavioral pharmacology, revealed that cyclic guanosine monophosphate acts as a second messenger in the dermal photoreceptor. Furthermore, gastropods possess dermal photoreceptors containing rhodopsin, as a photopigment, and another photosensitive protein, arrestin, responsible for terminating the light response. Thus, we chose three antibodies, anti-cGMP, anti-rhodopsin, and anti-β-arrestin, to identify the dermal photoreceptor molecules in *Lymnaea* mantle. Extracellular recording, using a suction electrode on the mantle, revealed a light off-response from the right parietal nerve. Overlapping structures, positive against each of the antibodies, were also observed. Numerous round, granular particles of 3–47 µm in diameter with one nucleus were distributed around pneumostome and/or inside the mantle. The cells surrounding the pneumostome area, located 10 µm beneath the surface, tended to have smaller cell soma ranging from 3 to 25 µm in diameter, while cells located in other areas were distributed uniformly inside the mantle, with a larger diameter ranging from 12 to 47 µm. The histological examination using back-filing Lucifer Yellow staining of the right parietal nerve with the three dermal photoreceptor antibodies confirmed that these overlapping-stained structures were dermal photoreceptors in *Lymnaea*.

Key words: immunohistochemistry, electrophysiology, extracellular recording, rhodopsin, cGMP, β arrestin

Extra-ocular photoreception is one of the essential sensory receptions developed during animal evolution, playing an important role in the regulation of diverse functions, such as biorhythms, reproduction, thermoregulation, bioluminescence, predator avoidance and learning and memory[1–6]. Dermal photoreceptors in mollusks are involved in the generation of circadian rhythms and escape behaviors[7–10]; however, the characteristics of morphological and physiological correspondence are not well understood[11]. The pulmonate fresh water pond snail, *Lymnaea stagnalis* has dermal photoreceptors, which mediate escape from predators through the whole-body withdrawal response, which is the only vigilance behavior available to this animal based on behavioral and physiological observations[9,12]. Snails respond to a

Abbreviations: **BSA**, bovine serum albumin; **BSCD**, buffered saline for color development; **CNG**, cyclic nucleotide-gated; **cGMP**, cyclic guanosine monophosphate; **DAB**, diaminobenzidine tetrahydrochloride; **IP_3**, inositol 1,4,5-triphosphate; **LED**, light emission diode; **LPeD11**, left pedal dorsal 11 neuron; **PBS**, phosphate buffered saline; **PBST**, phosphate buffered saline containing Triton X; **RPD1**, right parietal dorsal 1 neuron; **RPeD11**, right pedal dorsal 11 neuron; **TRP**, transient receptor potential

Corresponding author: Manabu Sakakibara, Laboratory of Neurobiological Engineering, School of High-Technology for Human Welfare, Tokai University, Numazu, Shizuoka 410-0321, Japan.
e-mail: manabu@tokai.ac.jp

shadow presentation, which mimics a predator attack through dermal photoreceptors sensing, conveying alert signals to the Right- and Left- Pedal Dorsal 11 neurons (RPeD11 and LPeD11), with chemical mono-synaptic connection to motor neurons[13–16], to evoke escape behavior through whole-body withdrawal. Thus, we can estimate the dermal photoreceptor response indirectly through the light-off response from RPeD11.

The photo-sensitive sensory receptor is divided into two types based on the second messenger or the channel involved. One sensory receptor type is the vertebrate ciliary photoreceptor cell, characterized by a hyperpolarizing response to a flash of light presentation involving cyclic nucleotide-gated (CNG) channels (Wensel, 2008). The other type of sensory receptor is the rhabdomeric photoreceptor cell in invertebrates, characterized by a depolarizing photoresponse through the generation of inositol 1,4,5-triphosphate (IP_3), resulting in the opening of a transient receptor potential (TRP) channel[17–20].

Our previous study demonstrated that *Lymnaea* possess both TRP channel-mediated ocular photoreceptor cells and CNG channel-mediated non-ocular photoreceptors distributed around the mantle and foot[13,18]. In the gastropod molluscan visual system, CNG and/or TRP channels also synergistically coexist in other than *Lymnaea*, such as *Onchidium*. The marine gastropod, *Onchidium verruculatum* has both extra-ocular and dermal photoreceptors located in the dorsal eye and stalk eye[21–24]. Rhodopsin-like photopigments in the extra-ocular photoreceptors of *Onchidium* were immunohistologically examined[22]. The photo-sensitive molecule, arrestin, responsible for terminating the light response, was recently electrophysiologically identified in ciliary photoreceptors in mollusks, and this molecule was further demonstrated to have an amino acid sequence identical to that of the mammalian β-arrestin[25].

In the present study we immunohistologically identified the dermal photoreceptors distributed in the mantle in *Lymnaea stagnalis* using 3 antibodies previously identified in molluscan photoreceptors: anti-cGMP, anti-octopus rhodopsin and anti-β-arrestin. This identity of these dermal receptors was further confirmed through an examination of the electrophysiological photoresponse of this snail.

Materials and Methods

Animals

Laboratory-reared fresh water pond snails, *Lymnaea stagnalis*, with shell lengths of 25–30 mm, were maintained at 22–24°C in well-aerated fresh water under a 12-h light: 12-h dark cycle (on at 08:00). The animals were maintained on a diet of cabbage and goldfish pellets.

Preparations and Immunohistochemistry

The mantle of a snail dark-adapted for more than 5 h was dissected under dim red (λ: 617 nm) LED illumination under anesthesia using 1-phenoxy-2-propanol, 0.125% diluted with *Lymnaea* saline (51.3 mM NaCl; 1.7 mM KCl; 4.1 mM $CaCl_2$; 1.5 mM $MgCl_2$; 5.0 mM HEPES, pH 7.9–8.1)[26]. An isolated mantle was fixed in 4% paraformaldehyde, diluted in 0.1 M phosphate buffer, pH 7.5, for 24 to 48 h, dehydrated in an ethanol series, and embedded in paraffin. Serial sections of 5 to 20 μm thick were cut vertically using a microtome (ERM-1017, Erma Inc., Tokyo, Japan). The thin paraffin sections were washed thoroughly with phosphate-buffered saline (PBS). For a 50-μm thick section, a fixed preparation was embedded in a 5% agar block, diluted in 10 mM PBS, and subsequently cut using a vibratome (VT-1000S, Leica Inc., Tubingen, Germany). To facilitate the antibody reaction, thin serial sections, following deparafinization with xylene and hydrophilic operation with an ethanol series, were incubated in 10 mM citrate buffer, pH 6.0, and subsequently heated with a microwave oven for antigen activation. For antigen activation, the thick sections were incubated in Triton X-100 diluted to 2% in PBS for 72 h, followed by thorough washing three times with PBS (pH 7.5) containing 0.05% Triton X (PBST) for 10 min. Subsequently, the sections were treated with the endogenous peroxidase and alkaline phosphatase blocking solution, BLOXALL (Vector Laboratories Inc., Burlingame CA, USA), for 30 min at room temperature to minimize background staining, and subsequently the sections were blocked with PBST containing 10% goat or rabbit serum at 4°C for 2 h, followed by washing with PBST and processing for immunohistochemical observation. The following primary antibodies were used: Rabbit anti-cGMP poly-clonal antibody (Milipore: 09-101, Billerica, MA, USA), rabbit anti-octopus rhodopsin poly-clonal antibody (Cosmo Bio: LSL-LB-5509, Tokyo, Japan), and anti-human β arrestin-1 (N-19) poly-clonal antibody (Santa Cruz Biotechnology: SC-6389, Dallas, TX, USA). The preparations were incubated with each primary antibody at a 1:1000–2000 dilution in PBST containing 1% bovine serum albumin (BSA) at 4°C for 16 to 48 h. The preparations were washed 3 times in PBST for 10 min and incubated in a 1:200 dilution of biotin-labeled secondary antibody (goat anti-rabbit-IgG antibody: Vector Laboratories, Burlingame CA, USA) at 4°C for 2 to 24 h. An avidin-biotin-peroxidase complex reagent or avidin-biotinylated alkaline phosphatase complex was subsequently applied to the preparations at 4°C for 2 to 24 h.

For antibody detection using the avidin-biotinylated alkaline phosphatase complex after washing with PBST, the preparations were incubated in buffer solution for color development (BSCD: 100 mM Tris-HCl, pH 9.5, 10 mM levamisole, 100 mM NaCl, and 5 mM $MgCl_2$) for 30 min at room temperature, and subsequently 0.02% NBT/BCIP containing BSCD was applied to the preparations for color development.

For antibody detection using the avidin-biotin-peroxidase complex reagent after washing with a 50 mM Tris buffer solution, pH 7.6, the preparations were incubated with a

0.1% solution of 3,3′-diaminobenzidine tetrahydrochloride (DAB) diluted in Tris buffer or VIP (VIP substrate kit for peroxidase: Vector Laboratories) for 3 min at room temperature, and subsequently color development was terminated after washing with Tris buffer or PBST.

As a positive control, the rat retina and/or *Lymnaea* ocular eye were embedded in paraffin and processed for immunohistochemical analysis using the same procedure as described above. The immunohistochemical analysis of the mantle without primary antibody was performed as a negative control.

Double staining experiments of nuclear and immunohistochemical staining were performed using the same procedures described above, and the preparations were incubated in Mayer Hematoxylin solution for 10 min, followed by washing with water for 30 min.

For confirmation of specificity to the anti-β arrestin antibody, a blocking peptide (Santa Cruz Biotechnology: SC-6389P, Dallas, TX, USA) was used to inactivate the corresponding antibody. After incubation with the blocking peptide, the antibody-positive tissue was no longer positive after immunohistochemical analysis using the anti-β arrestin antibody.

Back-fill staining with fluorescent dye

The isolated mantle was pinned to a Silgard-coated dissection dish, and the cutting edge of the nerve bundle from the right parietal nerve was physically isolated in a Vaserin dam filled with 5% Lucifer Yellow solution. The preparation was incubated at 20°C for several days to allow the dye to spread throughout the right parietal nerve, followed by fixation with 4% paraformaldehyde in 0.1 M PB solution and examination under a fluorescence microscope (Optiphoto-2, Nikon, Tokyo, Japan). The fixed mantle was cut into 50 µm thick sections and immunohistologically examined through staining with anti-Lucifer Yellow antibody (A-5750, Molecular Probe, Eugene, OR, USA) as described above. Since we used anti-Lucifer Yellow antibody obtained from rabbit IgG, we used biotinylated anti-rabbit IgG and visualized with ABC complex as described above. The stained images were examined on glass slides under a microscope (Diaphoto-TMD, Nikon, Tokyo, Japan) and captured using a digital camera (EOS kiss X2, Canon, Tokyo, Japan).

Extracellular recording from a nerve bundle

The mantle was isolated in *Lymnaea* saline using fine forceps and microscissors and subsequently pinned to a Silgard-coated experimental chamber under dim red illumination to avoid light exposure minimally. The light response was recorded from the right parietal nerve using a suction glass electrode, with a tip diameter of 30–40 µm, filled with *Lymnaea* saline located at the entry point into the ganglion. The extracellular recordings were performed using a suction electrode from the right parietal nerve fiber and a reference electrode placed in surrounding *Lymnaea* saline through an amplifier (DAP-100F, Dia Medical Inc., Tokyo, Japan). The photoresponse was processed using 'Power Lab' software (AD Instrument Inc., Colorado Springs, CO, USA).

The timing of the 250 ms light-off stimulus was controlled from a 50 W Halogen tungsten lamp (HL-10D, Hoya-Schott, Tokyo, Japan) using a solenoid mechanical shutter (EC-601, Copal, Tokyo, Japan) placed in the light path. The background light to keep the preparation under mesopic or light adapted condition was illuminated for the entire preparation using a fiber-optic cable. The maximum light intensity used to illuminate the preparation was ~700 µWcm^{-2} at 510 nm, recorded using a photopower meter (TQ8210, Advantest, Tokyo, Japan), using 1/10 attenuated white light through neutral density filters as the background illumination intermittent with a 250 ms light-off stimulus every 8 s.

Results

Immunohistochemical detection of dermal photoreceptors

To confirm that the immunoreactivity of the three antibodies was appropriately sensitive to detect the photo-sensitive cells, we performed immunohistological examination using the rat retina as a positive control. We observed that the area at the outer segment of rods was immunopositive to rhodopsin antibody; the outer segment of photoreceptor layer, inner plexiform layer, ganglion cell layer was immunopositive to cGMP antibody; and the inner- and outer-segment of the photoreceptor layer was immunopositive to β-arrestin antibody (data not shown). These findings were consistent with previous observations[27–31].

Structures positive to anti-rhodopsin antibody

Numerous tissues positive to anti-rhodopsin antibody were observed in the serial sections from the mantle in every case examined (n=8), as shown in Figure 1-A. The round-shaped, stained structure was 5 to 40 µm in diameter, comprising numerous granular clusters, densely stained with the anti-rhodopsin antibody in the cytoplasm (Fig. 1-C). An analysis of the 50 µm thick section revealed numerous granular clusters within the structure (Fig. 1-D). The image obtained from double staining with both anti-rhodopsin antibody and nuclear staining showed the presence of a single nucleus within the cytoplasm. This structure was confirmed as a single cell, as indicated with the white arrows in Figure 1-E. These cells were distributed almost uniformly from the surface to inner part of the mantle, as shown in Figure 1-A.

The pneumostome opening in *Lymnaea* was located in the right portion of the mantle, as shown in Figure 2-A. There were tissues positive to the anti-rhodopsin antibody in the pneumostome area surrounding the mantle (Fig. 2-B), while no staining was detected in the negative control sections (Fig. 2-C). The tissues positive to the antibody was also round-shaped structures of 5 to 20 µm in diameter, comprising numerous granular clusters at a depth of 10 to 100 µm from the surface, with one nucleus. The double staining experiment using both anti-rhodopsin antibody and nuclear

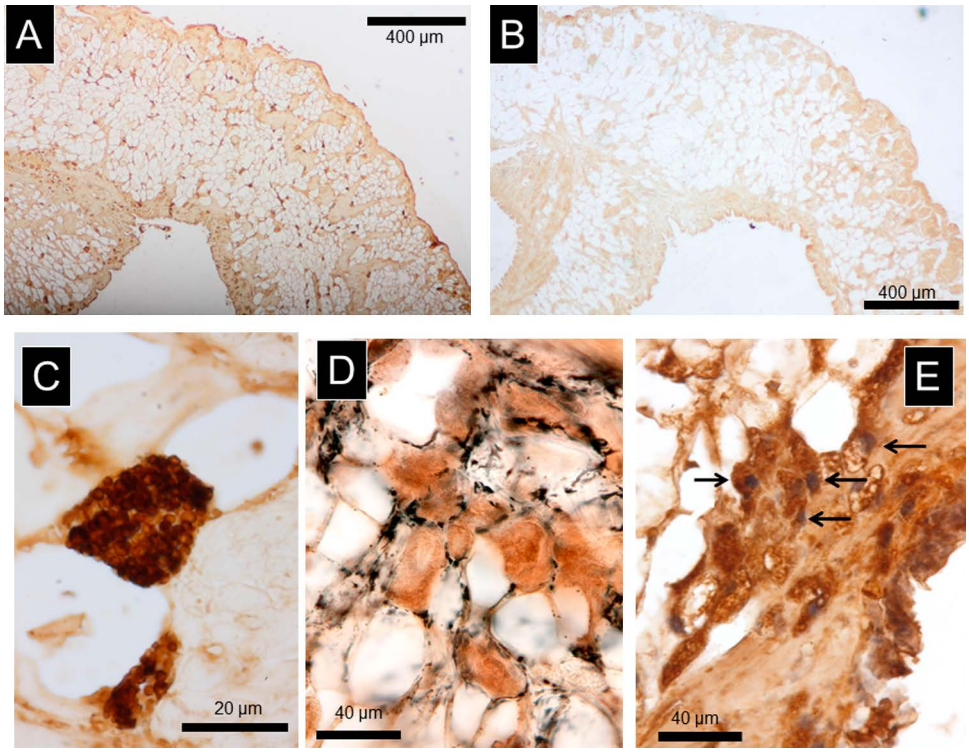

Figure 1 A) An image of the structures positive to anti-rhodopsin antibody in the mantle. Note that the antibody-positive structures were uniformly distributed throughout the section from top to bottom. The sections were cut vertically from the dorsal side to the ventral side. B) The negative control image without primary antibody staining. C) Enlarged image of the structures positive to the antibody. Note that there were numerous granular clusters inside the cell. D) Images of the structures positive to the antibody, observed in the 50 µm thick section. With this thick section, we could easily observe the numerous granular clusters. E) Double stained image using anti-rhodopsin antibody and nuclear staining. The nucleus was observed inside the structure, as indicated with arrows.

staining demonstrated the presence of a single nucleus inside each structure, indicating that these structures were cells, as indicated with arrows in Figure 2-D. The cells surrounding the pneumostome were characterized in smaller soma compared with those in the other mantle.

No structure was detected in the serial sections of the negative control without primary antibody (Fig. 1-B, Fig. 2-C), confirming that the stained tissue was the antibody specific.

As our previous study demonstrated that photo-transduction in *Lymnaea* ocular photoreceptor involves the TRP channel[18] and the spectral response curve from an ocular photoreceptor peaked at 480–500 nm, corresponding to the β_{max} of rhodopsin[32], we applied the anti-rhodopsin antibody to ocular eyes as a positive control (Fig. 3). The antibody showed immunopositivity for both the photoreceptor layer, as indicated with arrows, and the rhabdomeric membrane portion, as indicted with dashed-arrows (Fig. 3).

Structures positive to anti-β-arrestin and/or anti-cGMP antibodies

Both anti-β-arrestin (n=5) and anti-cGMP (n=5) antibodies showed immunoreactivity in the same structures surrounding the pneumostome area, as shown in Figure 4. The round shaped, antibody-positive structures were 5 to 40 µm in diameter, comprising numerous granules, distributed deep into the mantle (Fig. 4-B, -E) near the surface of the pneumostome opening (Fig. 4-C, -F). These structures were considered to be identical with those positive to the anti-rhodopsin antibody (Fig. 2). The specificity of the anti-β arrestin antibody was examined through incubation with the blocking peptide prior to immunostaining. Incubating the tissue with the blocking peptide inhibited immunopositivity to the anti-β arrestin antibody (data not shown). These findings confirmed that the anti β-arrestin antibody was specific to the tissues in paraffin-embedded sections. Furthermore, non-specific staining was observed without incubation with primary antibodies from the surface to less than 10 µm of pneumostome area, as shown in Figures 2-D, 4-C, 4-F. Hereafter, we excluded the non-specific cells positively stained with β arrestin and/or cGMP antibody from the surface to a 10-µm depth around the pneumostome area.

Contrasting results were obtained from the negative and positive control experiments. No tissues in the mantle sections were positively stained without anti-rhodopsin, anti-β-arrestin and anti-cGMP antibodies, whereas the area in the ocular eyes, i.e. photoreceptor soma layer and rhabdomeric

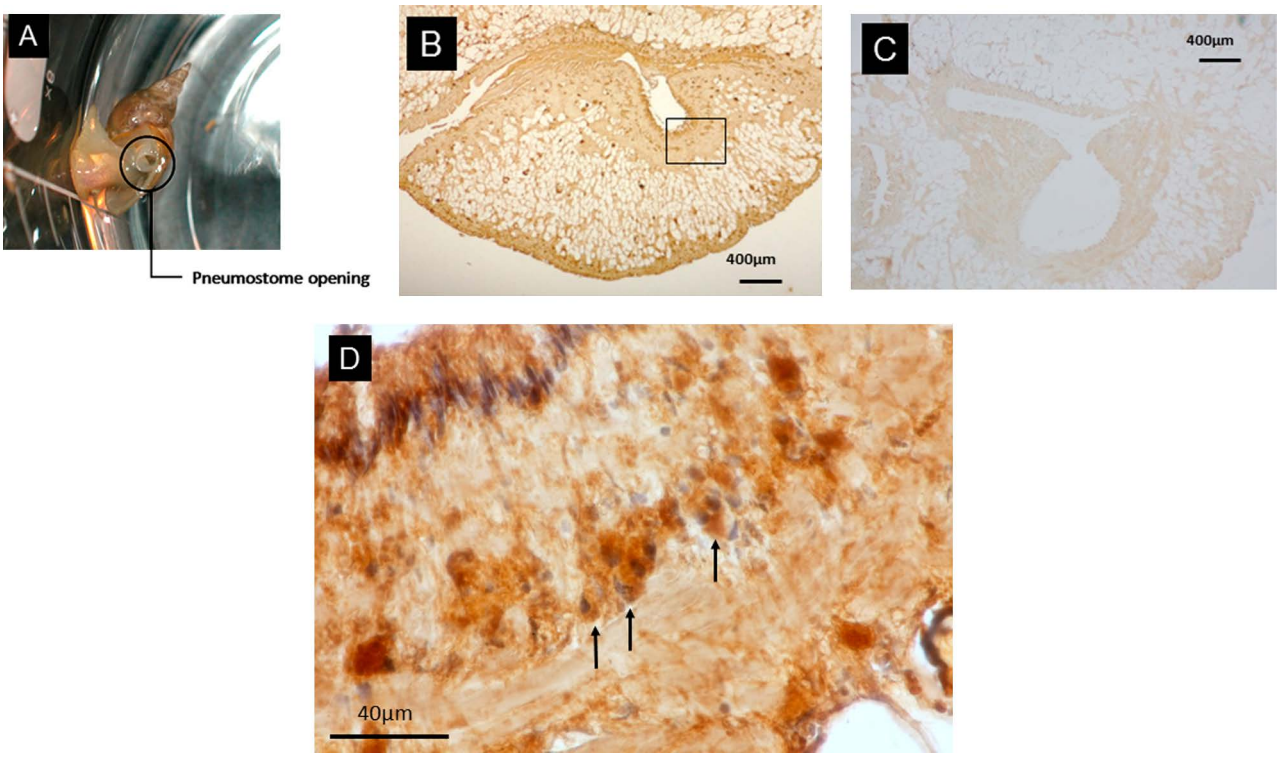

Figure 2 The structures around the pneumostome opening positive to anti-rhodopsin antibody. A) *Lymnaea* during breathing through the pneumostome. B) An image of the structures around pneumostome opening positive to anti-rhodopsin antibody. C) Negative control image without antibody staining. D) Enlarged image of the rectangular area in B), obtained through a double staining experiment using an antibody and nuclear staining. The cells with a single nucleus, comprising numerous granular clusters located at 10 to 100 µm beneath the surface, with cell bodies of 5 to 20 µm in diameter, as indicated with arrows.

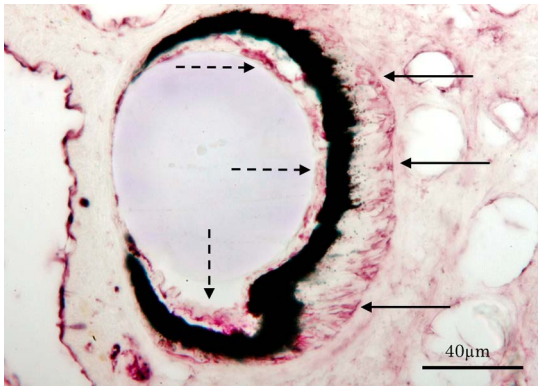

Figure 3 An ocular eye stained with the anti-rhodopsin antibody as a positive control. The section was made from the rostral (left) to the caudal (right) plane. The antibody positive area was observed at the rhabdomeric membranes (dashed-arrows) and photoreceptor somatic layers (arrows).

membrane area, was only positively stained for the anti-rhodopsin and β-arrestin antibodies, as shown in Figure 3, but no observable staining was detected in the same area for the cGMP antibody (data not shown).

Common antibody-positive areas in pairs of mirrored sections

The simultaneous staining of the same tissue divided into two symmetrical sections, as mirror images, was performed using anti-rhodopsin, anti-β-arrestin, and anti-cGMP antibodies.

The tissues positive to both anti-rhodopsin and anti-cGMP antibodies were detected in the pair of mirrored sections around pneumostome area. These structures comprised numerous granular clusters, as described above, showing immunopositivity against anti-rhodopsin and anti-cGMP antibodies (Fig. 5). The reactivity to anti-rhodopsin and anti-β-arrestin antibodies showed that the same area was positive to both antibodies (Fig. 6). In addition, positive areas to only anti-cGMP antibody were also detected, as indicated with dashed arrows (Fig. 5-B). Tissues positive to anti-rhodopsin and anti-β-arrestin antibodies were also observed; however, selective positive areas to the anti-β-arrestin antibody were also observed, as indicated with white dashed arrows (Fig. 6-B).

Taken together, these findings show that the three antibodies were positive for identical areas in the mantle. Notably, every area positive to each antibody was not always overlapped; structures that were not positive to anti-rhodopsin were positive to anti-cGMP and/or anti-β-arrestin antibod-

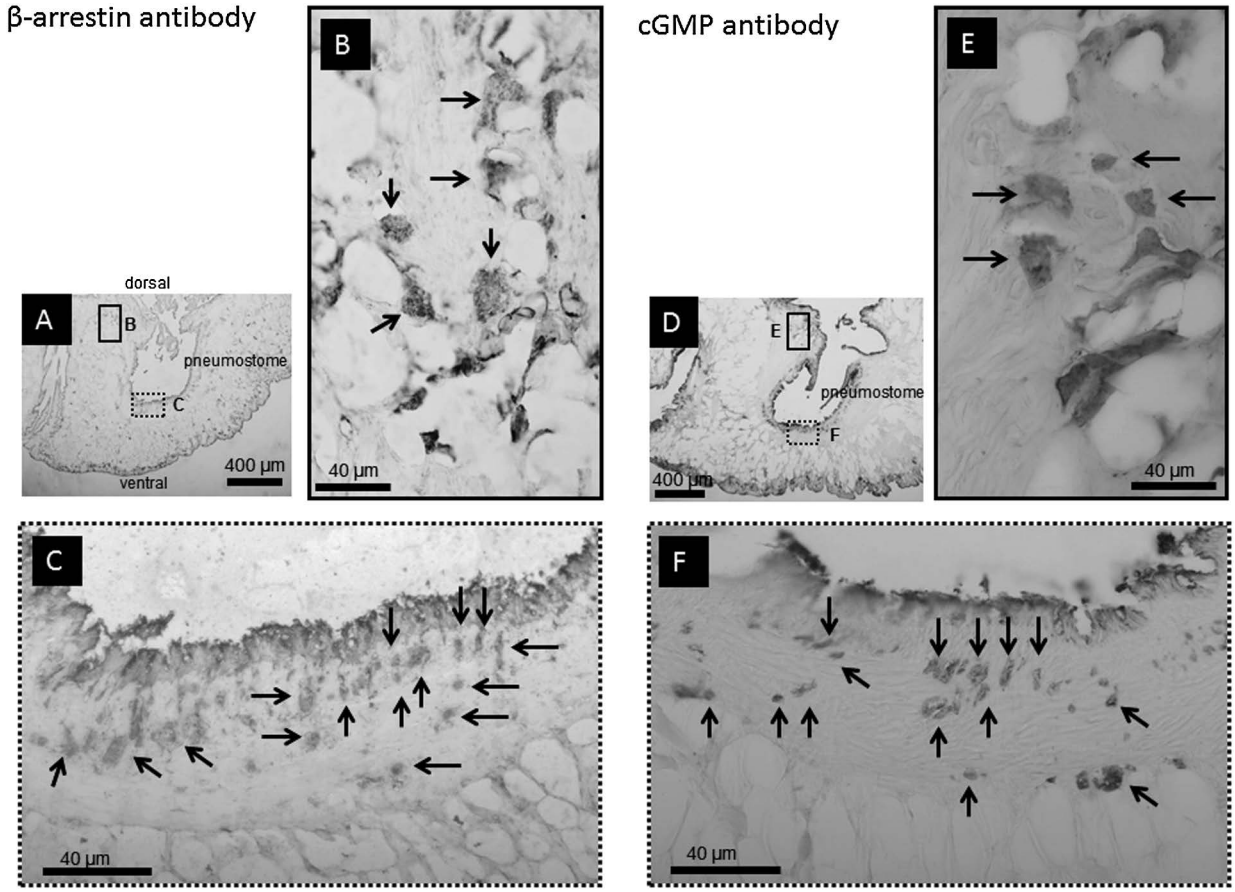

Figure 4 The tissues around pneumostome opening positive to the anti-β-arrestin (A, B, C) and anti-cGMP antibodies (D, E, F). A) An image of the anti-β-arrestin antibody-positive area. The enclosed rectangular images in B and C were enlarged. B) The antibody-positive structures of 20 to 40 μm in the soma diameter had numerous granular clusters and were distributed uniformly from the surface to bottom in the mantle, as indicated with arrows. C) The antibody-stained structures at the pneumostome opening, as indicated with arrows, were distributed from 10 μm beneath the surface. The dark area at the surface was not antibody specific. D) An image of the anti-cGMP antibody-positive area. The enclosed rectangular images in E and F were enlarged. E) The antibody-positive structures of 20 to 40 μm in diameter had numerous granular clusters and were distributed uniformly from the surface to bottom in the mantle as indicated with arrows. F) The antibody-stained structures at the pneumostome opening, as indicated with arrows, were distributed from 10 μm beneath the surface. The dark area at the surface was not antibody specific.

ies. The tissues positive to anti-β-arrestin and anti-cGMP antibodies showed that no granular clusters existed inside the cytosol.

Light-off response from the right parietal nerve

The results of a previous study suggested that photosensitive extra-ocular photoreceptors were present along the right parietal nerve fiber in the mantle[13]. In the present study, we examined whether the right parietal nerve located in the mantle was responsible for the light-off response. The extracellular recording electrode located on the mantle just the entering point to the central nervous system showed a photoresponse to light-off stimulus for 250 ms with several impulse generations, as shown in Figure 7. In response to three successive light-off stimuli, impulses were generated after stimulus with a 200–300 ms delay, as shown in Figure 7 in expanded time scale (lower column).

Detection of tissues in the right parietal nerve by back-filling method

An intracellular tracer dye, Lucifer Yellow, was detected in the mantle after incubation using the back-filling method for several days. The stained tissues were first observed using a fluorescence microscope and immunohistologically examined using anti-Lucifer Yellow antibody. The tissues positive to both the anti-rhodopsin and anti-Lucifer Yellow antibodies were detected around pneumostome area, showing round shape structures of 5 to 20 μm in diameter with a running axon, as shown in Figure 8-B. A thin, cylindrical-shaped structure of less than 1 μm in diameter was positive to the anti-Lucifer Yellow antibody, located at 10 to 100 μm from the surface. This structure resembled the tissue positive to the three antibodies previously described above.

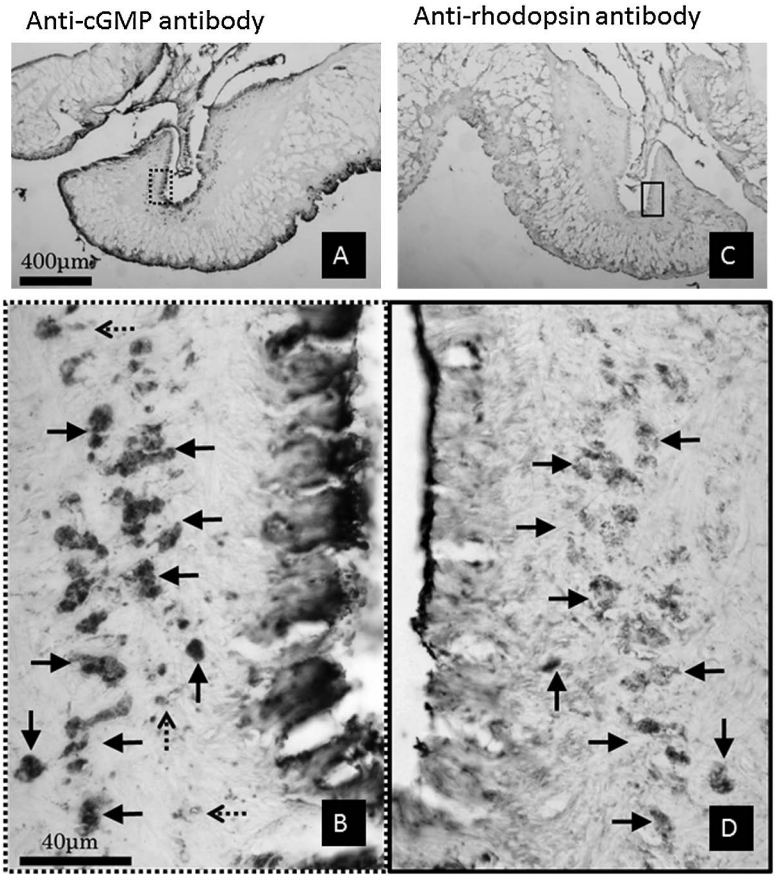

Figure 5 A pair of mirror images around the pneumostome opening stained with anti-cGMP (A, B) and anti-rhodopsin (C, D) antibodies. The calibration bars for A, C and B, D were identical. The enclosed rectangular areas were enlarged in B and D. The arrows in B and D correspond to the same structures; however, the 3 dashed-arrows in B were not detected with the anti-rhodopsin antibody. These structures were only positive to the anti-cGMP antibody.

Distribution of the cell size diameter in tissues positive to the three antibodies

The sizes of the cells positively stained against each antibodies in terms of area difference, i.e., pneumostome area or other area inside the mantle, is shown in Figure 9. The distribution histogram revealed that the smaller sized cells, ranging from 3 to 25 μm in diameter, were observed around pneumostome area (n=132; mean±standard deviation: 9.9±4.1 μm; median: 8.3 μm), whereas the cells located outside pneumostome area were larger in diameter, ranging from 12 to 47 μm (n=54; mean±standard deviation: 27.9±9.3 μm; median: 26.7 μm) and were positive against anti-rhodopsin antibody.

Discussion

In the present study, the dermal photoreceptors in *Lymnaea stagnalis* were immunohistologically and electrophysiologically studied. These cells in the mantle sections were immuno-positive to both anti-rhodopsin (n=8), anti-cGMP (n=5), and anti-β-arrestin (n=5) antibodies, characterized by a round shape of 3 to 47 μm in diameter. Every structure positive against one of three antibodies was not always positive to the other antibodies. Smaller cells of 3 to 25 μm in diameter tended to distribute around the pneumostome opening, at a depth of 10 to 100 μm beneath the surface. All dermal photoreceptors comprised numerous granular particles inside the cell. Extracellular recording, using a suction electrode from the right parietal nerve, revealed the light-off response, i.e., a shadow response with a 200 to 300 ms delay after the light-off stimulus.

Whether the dermal photoreceptors were located in the mantle where they make synapses to neurons in the central nervous system or the light sensitive tissue is the local periphery part of a neuron located in the central nervous system was still unclear. However our previous examination, that the withdrawal related inter neuron, RPeD11 received the "light off" response as shown in Figure 7 via one chemical synapse from dermal photoreceptors revealed by intracellular recordings from RPeD11, suggested the "light off" responses were likely from dermal photoreceptors located in the mantle by way of a chemical synapse[16]. This confirma-

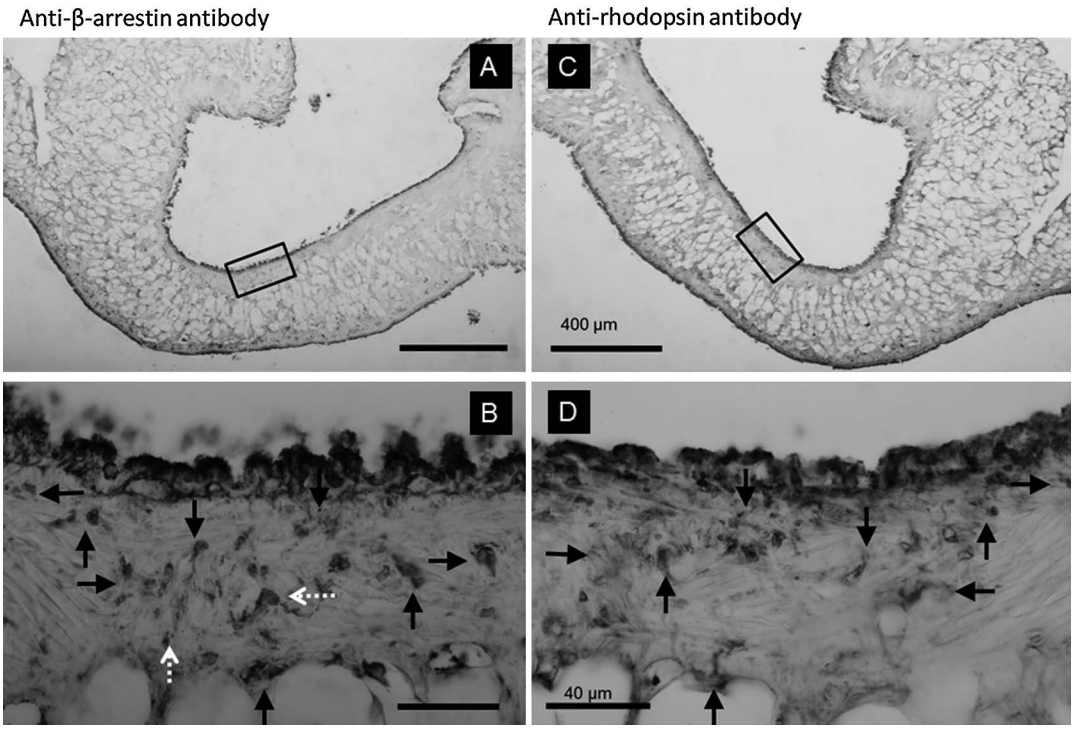

Figure 6 A pair of mirror images around pneumostome opening stained with anti-β-arrestin (A, B) and anti-rhodopsin (C, D) antibodies. The calibration bars for A, C and B, D were identical. The enclosed rectangular areas were enlarged in B and D. The arrows in B and D correspond to the same structures; however, the 2 white dashed-arrows in B were not detected with the anti-rhodopsin antibody. These structures were only positive to the anti-β-arrestin antibody.

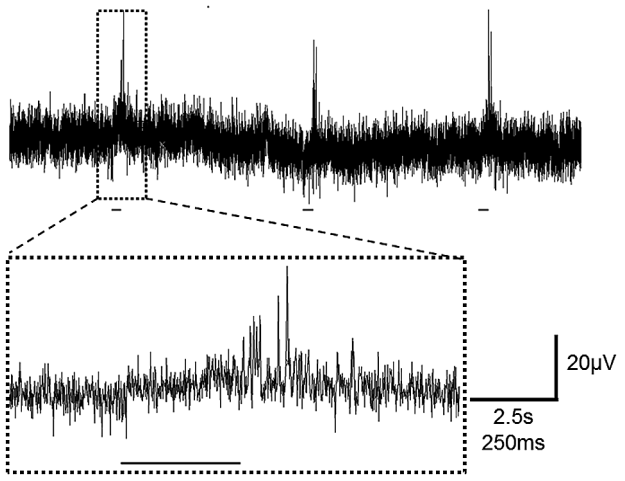

Figure 7 Light-induced response to light-off (pseudo shadow) stimuli. Extracellular recordings were made using a suction electrode from the right parietal nerve in the isolated mantle with pneumostome tissue. The upper trace indicates three successive light responses in a slower time scale (horizontal calibration bar corresponded to 2.5 s). A faster sweep recording (horizontal calibration bar corresponded to 250 ms) is shown in the lower column. The bars beneath each response indicated the timing of light off stimulus lasting for 250 ms. Note that the light-off stimulus induced impulse generations with 200 to 300 ms delay dependent on the background light intensity.

tion is left for the future study.

Previous studies demonstrated that membrane hyperpolarization occurs through a light-on response from RPeD11, which is the second-order neuron that receives multi-modal invasive sensory information, such as chemical, tactile and shadow information, resulting in escape behavior. All avoidance-related sensory receptor cells are distributed throughout the mantle or the foot to transmit information to the central nervous system via R- or L-PeD11[16]. Dermal photoreceptors are the one of the sensory receptors mediating the alert signal from a predator attack[14]. These receptors are completely independent on the ocular visual system, as a blind snail without ocular eyes could still detect shadow presentation, exhibiting whole-body withdrawal behavior, and photo-transduction in the dermal photoreceptor was mediated through cyclic nucleotide-gated (CNG) channel, as snails could not respond to shadow stimulus under the CNG channel blocker[13]. In *Drosophila*, the photo-sensitive molecule, rhodopsin, is photoisomerized upon photon absorption, leading to a reduction in the cGMP content, resulting in closure of the cGMP channel to block Na^+ inflow and induce hyperpolarization[33].

Thus, rhodopsin and cGMP were the good candidate molecules to detect dermal photoreceptors in *Lymnaea*. Another candidate for detection of dermal photoreceptors was β-arrestin. A recent study demonstrated that the terminating

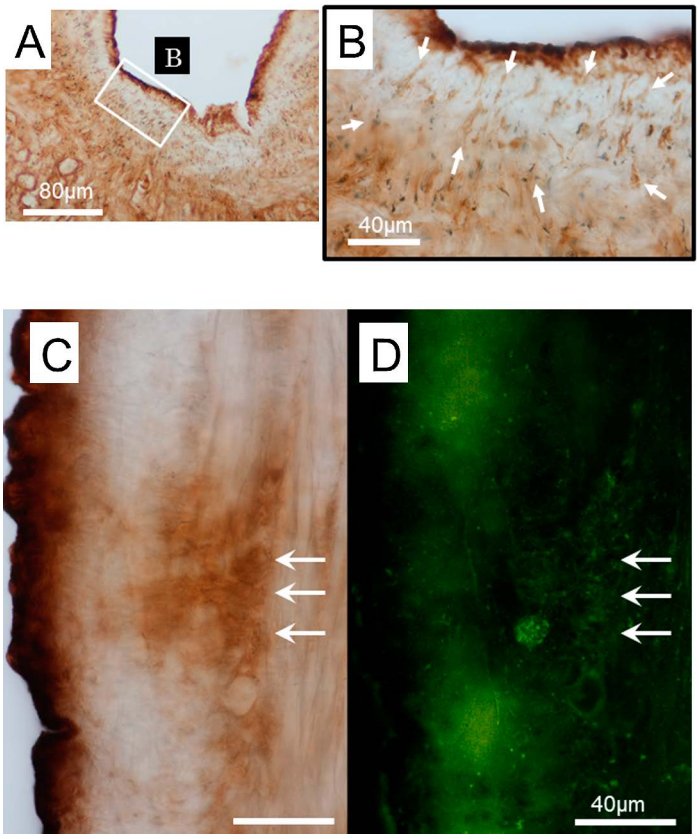

Figure 8 Dermal photoreceptor candidates stained using the backfill method. A tracer dye, Lucifer Yellow was back-filled from the nerve ending of the right parietal nerve and incubated for a couple of days, followed by processing with anti-Lucifer Yellow antibody. A) The Lucifer Yellow antibody-positive tissues were detected around the pneumostome opening, these tissues corresponded with the three antibodies, anti-rhodopsin, -β-arrestin, -cGMP antibody in the location and size. The enclosed rectangular area was enlarged in B. B) The white arrows indicate positivity to Lucifer Yellow antibody in the cell somas. C), D) An identical tissue was processed with anti-Lucifer Yellow antibody (C), and anti-rhodopsin antibody (D). The three arrows represent common positive areas to both antibodies.

the light response molecule, arrestin, existed in the photoreceptor of a scallop and comprised an amino acid sequence identical to that of mammalian β-arrestin[25]. We examined whether these three antibodies showed immunoreactivity against the dermal photoreceptors in *Lymnaea* and whether the photoresponse originating from the dermal photoreceptor could be electrophysiologically detected in the mantle.

Although the non-ocular visual system has been implicated in photo-tactic behavior under dim light[7,10], the underlying cellular mechanisms remain elusive. Our previous studies have demonstrated that the extra-ocular visual system is not involved in visuo-vestibular conditioning in *Lymnaea*[34,35], however a study of taste avoidance conditioning[36] revealed that withdrawal behavior was affected through shadow presentation, which mimicked the predator attack[16]. Furthermore, the saving period of long-term memory was dependent on the developmental stage of the snail[14].

Pedal neurons in *Hermissenda* are responsible for the light response originating from both ocular and non-ocular photoreceptors[37]. Although non-ocular photoreceptors have been ruled out as the source of the light response in *Hermissenda* pedal neurons[38], we examined the possibility to send information from the non-ocular visual system into parietal nerves. Parietal ganglion and right parietal dorsal 1 (RPD1) neurons have poly-modal sensory receptor input, including dermal photoreceptor input in *Lymnaea*[39] and the non-ocular dermal photoreception system in the foot, independent of the photoreceptor input from the eye[40]. Chono *et al.* 2002 reported that the light response from both sides of the inferior pedal nerves was characterized by the inhibitory response to light-on[40]; in another words, the impulse generation following the light-off stimulation could be recorded when a light-off stimulus is applied under continuous bright light. Consistently, in our previous study, we observed an off-response in RPeD11, from which the light response was indirectly observed via mono-synaptic chemical synapse[16]. Dermal photoreceptors in *Lymnaea* are located along the course of the axon running in the right parietal nerve, as confirmed through extracellular recordings and backfill tracer experiments.

Our previous studies have suggested that the ocular pho-

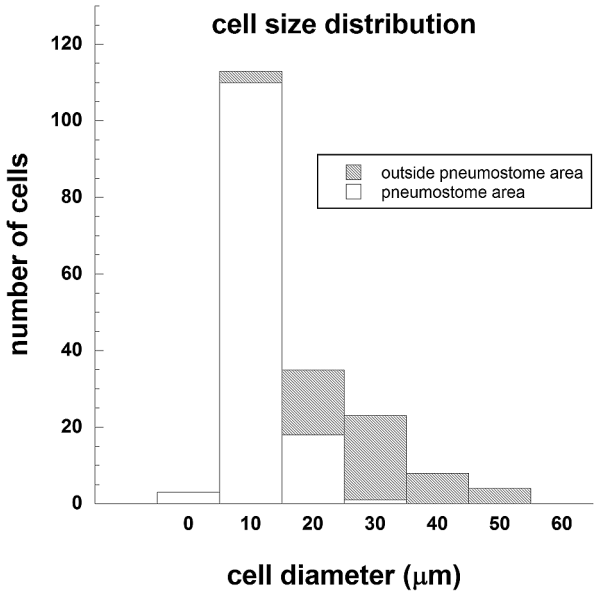

Figure 9 Distribution of cell sizes between the pneumostome area and the other areas. The cells were immune-positive to anti rhodopsin antibody.

toreceptor in *Lymnaea* was selectively responsible for the depolarizing photoresponse through TRP channels. In the present study, we did not detect any positive cells using the anti-cGMP antibody in the sections of ocular photoreceptor, consistent with our previous studies[18,32]. This evidence suggested that no cGMP-mediated channel was involved in ocular photoreception. Furthermore, the results obtained in the present study showed that every cell positive against each antibody was not always overlapped; thus, dermal photoreceptors in the mantle might play differentiated functions, such that different photo-sensitivity actions might be observed under dim light and/or bright light environments, or alternatively these photoreceptors might control photosensitivity itself.

Dermal photoreceptors of various sizes have been previously observed in *Onchidium*, ranging from 5 to 150 μm in diameter[41]. Consistent with the previous data, we showed that there were at least two classes of dermal photoreceptors in *Lymnaea*: smaller cells of 5 to 20 μm in diameter distributed around pneumostome area and larger cells of 20 to 50 μm in soma diameter distributed in area other than the pneumostome. These cells were commonly comprised numerous granular clusters inside the cell body, as shown in Figure 1-C. Both ciliary (cGMP dependent channel involved type) and rhabdomeric (TRP channel involved type) photoreceptors were immunopositive to anti-rhodopsin antibody in *Onchidium* dermal photoreceptors[41].

Arrestin is expressed in both types of photoreceptors for photo-transduction scallop[25] and horseshoe crab photoreceptors[42,43]. In the present study, we confirmed the expression of arrestin in the dermal photoreceptor in the mantle of *Lymnaea*. Arrestin has been implicated in both chemosensory transduction and phototransduction in some anthropoda[44]. The dual role for arrestin might be likely in cells pairs with mirror images of sections positive against anti-β-arrestin antibody but negative to anti-rhodopsin antibody, as shown in Figure 6-B. We also observed selective staining in a pair of mirror images between cGMP and rhodopsin antibodies; additional anti-cGMP antibody-positive cells were observed, which were not positive to rhodopsin antibody (Fig. 5-B). These cells contained no granular clusters inside the cytosol. The additional detection using anti-β arrestin and anti-cGMP antibodies might correspond to chemosensory receptors or mechanosensory receptors distributed throughout the mantle. Consistent with this notion, a recent study demonstrated that chemosensory, mechanosensory and photosensory receptors are present in the *Lymnaea* mantle[26].

Our previous study suggested that the axon of dermal photoreceptors are present throughout the anal and/or the genital nerves to the right internal and external nerve fibers that send afferent invasive information to the right parietal ganglion[16]. In the present study, we demonstrated that the photoresponse from the right parietal nerve endings in immune-positive cells was initiated from dermal photoreceptors.

Conclusion

Non-ocular dermal photoreceptors, responsible for light-off response, were identified using three antibodies, anti-rhodopsin, anti-cGMP, and anti-β-arrestin, in the mantle of *Lymnaea stagnalis*. The structures positive for each antibodies contained one nucleus, comprising granular particles located around a pneumostome at 10 μm beneath the surface and other areas inside the mantle. The cells around the pneumostome were characterized as smaller cells of 3 to 25 μm in diameter, while the cells in other areas were larger, ranging from 12 to 47 μm in diameter. Among the dermal photoreceptors in the mantle, we detected a light response from the right parietal nerve, physiologically characterized through an off-response and a morphological tracer dye using the backfill method and simultaneous staining with the anti-rhodopsin antibody.

References

1. Arikawa, K., Uchimi, K. & Eguchi, E. Extraocular photoreceptors in tha last abdominal ganglion of a swallowtail butterfly. *Natur wissenschaften* **78**, 82–84 (1991).
2. Fernald, R. D. Evolving eyes. *Int. J. Dev. Biol*. **48**, 701–705 (2004).
3. Horne, J. & Renninger, G. Circadian photoreceptor organs in *Limulus*. *J. Comp. Physiol. A*. **162**, 133–140 (1988).
4. Yamashita, H. & Tateda, H. Cerebral photosensitive neurons in the orb weaving spiders *Argiope bruennchii* and *A. amoena*. *J. Comp. Physiol. A*. **150**, 467–472 (1986).
5. Yoshida, M. ed. Extraocular photoreception. in *Hand book of Sensory Physiology*. (Autrum, H. ed.) pp. 581–640 (Springer, Berlin, 1979).

6. Young, R., Roper, C. & Walters, J. Eyes and extraocular photoreceptors in midwater cephalods and fishes. *Mol. Biol.* **15**, 371–380 (1979).
7. Duivenboden, Y. A. Non-ocular photoreceptors and photoorientation in the pond snail *Lymnaea stagnalis*. *J. Comp. Physiol. A*. **149**, 363–368 (1982).
8. Lukowiak, K. & Jacklet, J. W. Habituation and dishabituation: interactions between peripheral and central nervous systems in *Aplysia*. *Science* **178**, 1306–1308 (1972).
9. Stoll, C. J. Sensory systems involved in the shadow response of *Lymnaea stagnalis*. *Proc. K. Ned. Akad. Wet. C* **75**, 342–351 (1972).
10. Stoll, C. J. On the role of eyes and non-ocular light receptors in orientational behaviour of *Lymnaea stagnalis* (L.). *Proc. K. Ned. Akad. Wet. C* **76**, 203–214 (1973).
11. Steven, D. M. The dermal light sense. *Biol. Rev. Camb. Philos. Soc*. **38**, 204–240 (1963).
12. Ferguson, G. P. & Benjamin, P. R. The whole-body withdrawal response of *Lymnaea stagnalis*. II. Activation of central motoneurones and muscles by sensory input. *J. Exp. Biol.* **158**, 97–116 (1991).
13. Pankey, S., Sunada, H., Horikoshi, T. & Sakakibara, M. Cyclic nucleotide-gated channels are involved in phototransduction of dermal photoreceptors in *Lymnaea stagnalis*. *J. Comp. Physiol. B*. **180**, 1205–1211 (2010).
14. Sunada, H., Horikoshi, T., Lukowiak, K. & Sakakibara, M. Increase in excitability of RPeD11 results in memory enhancement of juvenile and adult of *Lymnaea stagnalis* by predator-induced stress. *Neurobiol. Learn. Mem*. **94**, 269–277 (2010).
15. Inoue, T., Takasaki, M., Lukowiak, K. & Syed, N. I. Identification of a putative mechanosensory neuron in *Lymnaea*: characterization of its synaptic and functional connections with the whole-body withdrawal interneuron. *J. Neurophysiol*. **76**, 3230–3238 (1996).
16. Sunada, H., Sakaguchi, T., Horikoshi, T., Lukowiak, K. & Sakakibara, M. The shadow-withdrawal response, dermal photoreceptors and their input to a higher order interneuron, RPeD11 in the pond snail *Lymnaea stagnalis*. *J. Exp. Biol*. **213**, 3409–3415 (2010).
17. Minke, B. The history of the *Drosophila* TRP channel: the birth of a new channel superfamily. *J. Neurogenet*. **24**, 216–233 (2010).
18. Sakakibara, M. Comparative study of visuo-vestibular conditioning in *Lymnaea stagnalis*. *Biol. Bull*. **210**, 298–307 (2006).
19. Sakakibara, M., Inoue, H. & Yoshioka, T. Evidence for the involvement of inositol trisphosphate but not cyclic nucleotides in visual transduction in *Hermissenda* eye. *J. Biol. Chem*. **273**, 20795–20801 (1998).
20. Sakakibara, M., Alkon, D. L., Kouchi, T., Inoue, H. & Yoshioka, T. Induction of photoresponse by the hydrolysis of polyphosphoinositides in the *Hermissenda* type B photoreceptor. *Biochem. Biophys. Res. Commun.* **202**, 299–306 (1994).
21. Gotow, T. & Nishi, T. Simple photoreceptors in some invertebrates: physiological properties of a new photosensory modality. *Brain Res*. **1225**, 3–16 (2008).
22. Katagiri, N., Terakita, A., Shichida, Y. & Katagiri, Y. Demonstration of a rhodopsin-retinochrome system in the stalk eye of a marine gastropod, *Onchidium*, by immunohistochemistry. *J. Comp. Neurol*. **433**, 380–389 (2001).
23. Katagiri, N., Suzuki, T., Shimatani, Y. & Katagiri, Y. Localization of retinal proteins in the stalk and dorsal eyes of the marine gastropod, *Onchidium*. *Zoolog. Sci*. **19**, 1231–1240 (2002).
24. Nishi, T. & Gotow, T. Light-increased cGMP and K^+ conductance in the hyperpolarizing receptor potential of *Onchidium* extra-ocular photoreceptors. *Brain Res*. **809**, 325–336 (1998).
25. Gomez, M., Espinosa, L., Ramirez, N. & Nasi, E. Arrestin in ciliary invertebrate photoreceptors: molecular identification and functional analysis in vivo. *J. Neurosci*. **31**, 1811–1819 (2011).
26. Wyeth, R. C. & Croll, R. P. Peripheral sensory cells in the cephalic sensory organs of *Lymnaea stagnalis*. *J. Comp. Neurol*. **519**, 1894–1913 (2011).
27. Shallal, A., Mckechnie, N. M. & Al-Mahdawi, S. Immunochemistry of the outer retina. *Eye (Lond)* **2**, S180–201 (1988).
28. Mendez, A., Lem, J., Simon, M. & Chen, J. Light-dependent translocation of arrestin in the absence of rhodopsin phosphorylation and transducin signaling. *J. Neurosci*. **23**, 3124–3129 (2003).
29. Nair, K. S., Hanson, S. M., Mendez, A., Gurevich, E. V., Kennedy, M. J., Shestopalov, V. I., Vishnivetskiy, S. A., Chen, J., Hurley, J. B., Gurevich, V. V. & Slepak, V. Z. Light-dependent redistribution of arrestin in vertebrate rods is an energy-independent process governed by protein-protein interactions. *Neuron* **46**, 555–567 (2005).
30. Gamm, D. M., Barthel, L. K., Raymond, P. A. & Uhler, M. D. Localization of cGMP-dependent protein kinase isoforms in mouse eye. *Invest. Ophthalmol. Vis. Sci*. **41**, 2766–2773 (2000).
31. Ortez, R. A., Sikes, R. W. & Sperling, H. G. Immunohistochemical localization of cyclic GMP in goldfish retina. *J. Histochem. Cytochem*. **28**, 263–270 (1980).
32. Sakakibara, M., Aritaka, T., Iizuka, A., Suzuki, H., Horikoshi, T. & Lukowiak, K. Electrophysiological responses to light of neurons in the eye and statocyst of *Lymnaea stagnalis*. *J. Neurophysiol*. 93, 493–507 (2005).
33. Hardie, R. C. Phototransduction mechanisms in *Drosophila* microvillar photoreceptors. *WIRs: Membrane Transport and Signaling* **1**, 162–187 (2012).
34. Sakakibara, M., Kawai, R., Kobayashi, S. & Horikoshi, T. Associative learning of visual and vestibular stimuli in *Lymnaea*. *Neurobiol. Learn. Mem*. **69**, 1–12 (1998).
35. Ono, M., Kawai, R., Horikoshi, T., Yasuoka, T. & Sakakibara, M. Associative Learning Acquisition and Retention Depends on Developmental Stage in *Lymnaea stagnalis*. *Neurobiol. Learn. Mem*. **78**, 53–64 (2002).
36. Kawai, R., Sunada, H., Horikoshi, T. & Sakakibara, M. Conditioned taste aversion with sucrose and tactile stimuli in the pond snail *Lymnaea stagnalis*. *Neurobiol. Learn. Mem*. **82**, 164–168 (2004).
37. Jerussi, T. P. & Alkon, D. L. Ocular and extraocular responses of identifiable neurons in pedal ganglia of *Hermissenda crassicornis*. *J. Neurophysiol*. **46**, 659–671 (1981).
38. Hodgson, T. M. & Crow, T. Characterization of 4 light-responsive putative motor neurons in the pedal ganglia of *Hermissenda crassicornis*. *Brain Res*. **557**, 255–264 (1991).
39. Zaitsev, O. V. & Shuvalova, N. E. Morphologic characteristics of the RPDI neuron in the pond snail and its participation in the processing of multimodality sensory information. *Neirofiziologiia* **20**, 785–793 (1988).
40. Chono, K., Fujito, Y. & Ito, E. Non-ocular dermal photoreception in the pond snail *Lymnaea stagnalis*. *Brain Res*. **951**, 107–112 (2002).
41. Katagiri, N. & Katagiri, Y. A multiple photoreceptive system in a marine gastropod, *Onchidium*: 1) Morphological characteristics and photoresponse of four kinds of photoreceptor cells. *Hikaku seiri seikagaku (Comparative Physiology and Biochemistry)* **25**, 4–10 (2008).
42. Sacunas, R. B., Papuga, M. O., Malone, M. A., Pearson, A. C., Jr., Marjanovic, M., Stroope, D. G., Weiner, W. W., Chamberlain, S. C. & Battelle, B. A. Multiple mechanisms of rhabdom shedding in the lateral eye of *Limulus polyphemus*. *J. Comp. Neurol*. **449**, 26–42 (2002).
43. Battelle, B. A., Dabdoub, A., Malone, M. A., Andrews, A. W.,

Cacciatore, C., Calman, B. G., Smith, W. C. & Payne, R. Immunocytochemical localization of opsin, visual arrestin, myosin III, and calmodulin in *Limulus* lateral eye retinular cells and ventral photoreceptors. *J. Comp. Neurol*. **435**, 211–225 (2001).

44. Merrill, C. E., Riesgo-Escovar, J., Pitts, R. J., Kafatos, F. C., Carlson, J. R. & Zwiebel, L. J. Visual arrestins in olfactory pathways of *Drosophila* and the malaria vector mosquito *Anopheles gambiae*. *Proc. Natl. Acad. Sci. USA* **99**, 1633–1638 (2002).